0022-3565/03/3061-84–92$7.00
THE JOURNAL OF PHARMACOLOGY AND EXPERIMENTAL THERAPEUTICS
JPET 306:84–92, 2003

Vol. 306, No. 1
49809/1069699
Printed in U.S.A.

Amide Local Anesthetics Potently Inhibit the Human Tandem Pore Domain Background K^+ Channel TASK-2 (KCNK5)

CHRISTOPH H. KINDLER, MATTHIAS PAUL, HILARY ZOU, CANHUI LIU, BRUCE D. WINEGAR, ANDREW T. GRAY, and C. SPENCER YOST

Department of Anesthesia, University Clinics, Kantonsspital, Basel, Switzerland (C.H.K.); Department of Anesthesia and Operative Intensive Care Medicine, University of Köln, Köln, Germany (M.P.); and Department of Anesthesia and Perioperative Care, University of California, San Francisco, California (H.Z., C.L., B.D.W., A.T.G., C.S.Y.)

Received January 30, 2003; accepted March 17, 2003

ABSTRACT

Blockade of voltage-gated sodium (Na^+) channels by local anesthetics represents the main mechanism for inhibition of impulse propagation. Local anesthetic-induced potassium (K^+) channel inhibition is also known to influence transmission of sensory impulses and to potentiate inhibition. K^+ channels involved in this mechanism may belong to the emerging family of background tandem pore domain K^+ channels (2P K^+ channels). To determine more precisely the effects of local anesthetics on members of this ion channel family, we heterologously expressed the 2P K^+ channels TASK-2 (KCNK5), TASK-1 (KCNK3), and chimeric TASK-1/TASK-2 channels in oocytes of *Xenopus laevis.* TASK-2 cDNA-transfected HEK 293 cells were used for single-channel recordings. Local anesthetic inhibition of TASK-2 was dose-dependent, agent-specific, and stereoselective. The IC_{50} values for *R*-(+)-bupivacaine and *S*-(−)-bupivacaine were 17 and 43 μM and for *R*-(+)-ropivacaine and *S*-(−)-ropivacaine, 85 and 236 μM. Lidocaine (1 mM) inhibited TASK-2 currents by 55 ± 4%, whereas its quaternary positively charged analog *N*-ethyl lidocaine (QX314) had no effect. Bupivacaine (100 μM) decreased channel open probability from 20.8 ± 1.6% to 5.6 ± 2.2%. Local anesthetics [300 μM *R*-(+)-bupivacaine] caused significantly greater depolarization of the resting membrane potential of TASK-2-expressing oocytes compared with water-injected control oocytes (15.8 ± 2.5 mV versus 0.1 ± 0.05 mV; $p < 0.001$). Chimeric TASK-1/TASK-2 2P K^+ channel subunits that retained pH sensitivity demonstrated that the carboxy domain of TASK-2 mediates the greater local anesthetic sensitivity of TASK-2. These results show that clinically achievable concentrations of local anesthetics inhibit background K^+ channel function and may thereby enhance conduction blockade.

The molecular mechanisms of local anesthetic inhibition of voltage-gated sodium (Na^+) channels and the resulting blockade of propagation of compound action potentials are well described (Ragsdale et al., 1994). In addition to the recognized importance of Na^+ channel inhibition for peripheral and neuroaxial nerve block, other ion channels also contribute to local anesthetic action (Butterworth and Strichartz, 1990). Blockade of potassium (K^+) channels has been shown to potentiate local anesthetic-induced impulse inhibition (Drachman and Strichartz, 1991). Local anesthetics inhibit a number of heterologously expressed voltage-gated K^+ channels including hKv1.5, Kv2.1, Kv4.3, KvLQT1, and G protein-coupled inward rectifying K^+ channels at micromolar concentrations (González et al., 2001b; Zhou et al., 2001). In addition, local anesthetics inhibit K^+ currents in various neuronal preparations, including transient K^+ currents in rat dorsal horn neurons (Olschewski et al., 1998) and sustained K^+ currents in isolated rat dorsal root ganglion neurons (Komai and McDowell, 2001) and amphibian sciatic nerves (Bräu et al., 1998).

Local anesthetics are also potent inhibitors of the newly discovered third superfamily of K^+ channels, i.e., the tandem pore domain K^+ channels (2P K^+ channels) (Kindler et al., 1999). The 2P K^+ channels are named KCNK channels according to the HUGO Gene Nomenclature Committee (http://www.gene.ucl.ac.uk/nomenclature/genefamily/KCN.shtml). The structural orientation of these K^+ channel subunits probably consists of four transmembrane segments and two pore-forming domains in tandem within their primary amino acid sequence with amino and carboxyl (C) terminals arrayed

This research was supported by National Institutes of Health Grant GMS-51372 (C.S.Y.) and financial institutional resources from the Anesthesia Department, Kantonsspital, University Clinics, Basel (C.H.K.).
Article, publication date, and citation information can be found at http://jpet.aspetjournals.org.
DOI: 10.1124/jpet.103.049809.

ABBREVIATIONS: 2P, tandem pore domain; CNS, central nervous system; TASK, TWIK (tandem pore weak inward rectifying K channel)-related acid-sensitive K^+ channel; TOK, two pore domains outward-rectifying K^+ channel; TREK, TWIK-related K^+ channel; δ, fractional electrical distance; QX314, *N*-ethyl lidocaine; FR, frog Ringer's solution; n_H, Hill coefficient; PCR, polymerase chain reaction; pH_m, pH value for 50% of inhibition; P_o, open probability; τ, time constant of activation; IQB-9302, ciprocaine.

intracellularly (for review, see Goldstein et al., 2001). Most of these 2P K^+ channels are widely expressed in the central nervous system (CNS) (Talley et al., 2001), and their physiological role and function are emerging. They are believed to constitute the molecular entities of background or leak K^+ conductances involved in the control of the resting membrane potential and firing pattern of excitable cells; inhibition of these channels produces membrane depolarization (Eglen et al., 1999; Kindler et al., 1999). Thus, local anesthetics could potentiate impulse inhibition by blockade of these 2P K^+ channels. Local anesthetic-induced depolarization of the resting membrane potential of cells expressing these channels would promote formation of the open and inactivated states of voltage-gated Na^+ channels, thereby increasing the affinity of Na^+ channels for local anesthetics.

Moreover, inhibition of 2P K^+ channels also increases membrane excitability and may therefore contribute to the cardiotoxic and excitotoxic side effects of local anesthetics. The background K^+ conductances in cardiomyocytes (Aimond et al., 2000; Terrenoire et al., 2001) and cerebellar granule and Purkinje neurons (Millar et al., 2000; Bushell et al., 2002) are carried, at least in part, by 2P K^+ channels. Bupivacaine, which is the most toxic local anesthetic clinically used, inhibits the background 2P K^+ channels TASK-1 and TREK-1 (Kindler et al., 1999), both expressed in heart and CNS, at concentrations achieved with inadvertent intravascular injection (~20 μM) (Kotelko et al., 1984). Recently, it has been shown that blockade of TASK-1 currents is responsible for the arrhythmogenic effects of platelet-activating factor in murine ventricular myocytes (Barbuti et al., 2002). In the present study we examined the local anesthetic inhibition of the 2P K^+ channel TASK-2, which is expressed in heart and CNS (Gray et al., 2000; Gabriel et al., 2002), with special attention to both stereoselectivity and structure-activity relations. The typical local anesthetic molecule is a tertiary amine attached to a substituted aromatic ring by an intermediate chain containing either an ester or an amide linkage; local anesthetics are therefore classified as aminoester or aminoamide compounds. It has been shown that aminoester local anesthetics are more potent inhibitors of resting Na^+ channels and compound action potential than aminoamide compounds, whereas background K^+ channels are more resistant to ester-linked local anesthetics (Kindler et al., 1999).

Materials and Methods

Two-Electrode Voltage-Clamp Electrophysiological Recording and Analysis. The present study was approved by the Committee on Animal Research of the University of California, San Francisco. The methods of oocyte harvesting and injection of cRNA were performed as previously described (Kindler et al., 1999).

Lidocaine, racemic bupivacaine, tetracaine, benzocaine, and *N*-ethyl lidocaine (QX314) were purchased from Sigma-Aldrich (St. Louis, MO). *R*-(+)- and *S*-(−)-bupivacaine and *R*-(+)-, *S*-(−)-, and racemic ropivacaine were kindly provided by AstraZeneca Pharmaceuticals (Södertälje, Sweden). Stock solutions of local anesthetics were prepared in frog Ringer's solution (FR) (115 mM NaCl, 2.5 mM KCl, 1.8 mM $CaCl_2$, 10 mM HEPES, pH 7.6) and kept at 4°C for no more than 4 weeks. A stock solution of 1 M benzocaine in ethanol and 1 mM QX314 in FR were made up immediately before the experiments.

Oocytes were studied by two microelectrode voltage-clamp and current-clamp techniques using a GeneClamp 500B amplifier (Axon Instruments, Union City, CA). For the voltage-clamp experiments, the holding potential was −80 mV. Voltage pulse protocols used 1-s steps ranging from −140 to +40 mV in 20-mV increments, with 1.5-s interpulse intervals. Electrophysiological studies were performed at room temperature (20–23°C) in a 25-μl recording chamber perfused with FR at a rate of approximately 4 to 5 ml/min. Local anesthetic solutions were applied for 2 to 4 min before voltage pulse protocols, and washout experiments were performed after 2 to 4 min of superfusion with local anesthetic-free FR solution. For most experiments, current signals were low-pass-filtered with a four-pole Bessel filter at 50 to 100 Hz and sampled at 100 to 1000 Hz. Normalized responses of steady-state currents (at the depolarizing pulse of +40 mV pulse) with respect to control were calculated to give concentration-inhibition curves. The IC_{50} values, 95% confidence intervals, and Hill coefficients (n_H) for inhibition of TASK-2 currents were obtained from fitting the fractional block f ($f = 1 - I_{Drug}/I_{control}$) at various local anesthetic concentrations to the Hill equation using a nonlinear least-squares fitting procedure (Prism; GraphPad Software, Inc., San Diego, CA):

$$f = 1/[1 + (IC_{50}/[LA])^{n_H}]$$

where IC_{50} is drug concentration, where 50% inhibition is observed, [LA] is concentration of local anesthetic, and n_H is the Hill coefficient.

The voltage dependence of local anesthetic inhibition of TASK-2 currents was analyzed by normalization of leakage-subtracted currents in the presence of local anesthetic to matching controls, to yield a fractional block f at each voltage. Data at potentials greater than −60 mV were then fit to the Woodhull equation by regression (JMP Software; SAS Institute, Inc., Cary, NC) to estimate the Woodhull coefficient δ:

$$f = [LA]/([LA] + IC_{50(Em=0)} \times \exp(-\delta z F Em/RT))$$

where f is fractional block at each voltage, Em is membrane potential, z is valence, δ is the Woodhull coefficient (fraction of the electric field that the blocker experiences), and F, R, and T have their usual meanings in thermodynamics. For calculations of the Woodhull coefficient δ, the effective charge z was assumed to be +1.

The time constant (t) for TASK-2 activation was estimated by fitting it to the following one-phase exponential equation (Prism; GraphPad Software, Inc.):

$$y = C + A \times \exp(-\text{time}_{(s)}/\tau)$$

where τ is the time constant of activation, A is the amplitude of current, and C is the baseline value. To examine the activation of chimeric 2P K^+ channel subunits, the fractional instantaneous current (defined as the ratio of the instantaneous current at 150 ms divided by the steady-state current) was measured.

Except where stated otherwise, results are expressed as mean ± S.E.M. Comparisons between mean values of two variables were performed by unpaired Student's t test. Statistical significance was defined by $p < 0.05$. For each data point, results from 2 to 12 oocytes were analyzed, and at least two different batches of oocytes were used.

Expression of TASK-2 in HEK 293 Cells and Single-Channel Recording. Cultures of HEK 293 cells were maintained at 37°C in a 95% air, 5% CO_2 (v/v) humidified atmosphere. The cells were grown in Dulbecco's modified Eagle's media with high glucose concentration (4.5 g/l), 10% fetal bovine serum, penicillin 100 μg/ml, streptomycin 100 units/ml, and 2 mM glutamine. Cells were grown to 60 to 80% confluence and transfected with a pZeo vector (Invitrogen, Carlsbad, CA) that included the cDNA for TASK-2 (Gray et al., 2000). Cells were maintained in selection media that included 600 μg/ml Zeocin and used for experiments 24 to 48 h after transfection. Patch electrodes were pulled from borosilicate pipettes. The shanks were coated with Sylgard and the tips were heat polished. The recording micropipette resistances ranged from 3 to 6 MΩ, and seal resistances ranged from 5 to 20 GΩ. The electrode filling solution contained 150

mM potassium aspartate, 3 mM NaCl, 10 mM HEPES, 86 mM glucose, 1 mM EGTA, 5 mM $MgCl_2$ (pH 7.4). The bath solution contained 150 mM potassium aspartate, 10 mM HEPES, 3 mM NaCl, 14 mM glucose, 2 mM $CaCl_2$, and 5 mM $MgCl_2$ (pH 7.4). The experimental solutions were delivered to the cell at 20 μl/min. The perfusion rate was fast enough to allow undiluted perfusion of the cell. Perfusion with bathing solution alone had no effect on current amplitudes and other measures of channel activity. Single-channel currents were recorded with an Axopatch 200B amplifier (Axon Instruments, Inc.), filtered at 2 KHz, digitized at a sample rate of 100 μs with an InstruTECH ITC-16 A/D converter (InstruTECH, Port Washington, NY), and recorded to disk. Before seal formation, the voltage offset between the patch electrode and the bath solution was adjusted to produce zero current. Gigaohm seals were formed on cells, and they were perfused with aqueous solutions of bupivacaine. All experiments were performed at room temperature (20–23°C). Amplitude histograms were generated from current records of 100-s duration. The components of the amplitude distributions were fit to a multi-Gaussian probability density with the program TAC (Bruxton Corp., Seattle, WA). We assumed that all the channels in a multichannel patch gated independently and had the same open probability. The mean open probability was determined from the probability density by calculating the mean open-channel current amplitude divided by the single-channel current and the number of channels.

Construction of Chimeric 2P K^+ Channels. Two chimeric TASK-1/TASK-2 and TASK-2/TASK-1 subunits, named chimera1 and chimera2, were produced by sequential nested polymerase chain reaction (PCR) that swapped the carboxyl (C)-terminal domains of TASK-1 (amino acids 248–411) or TASK-2 (amino acids 251–499) to the other 2P K^+ channel. Primers were designed to amplify from plasmid DNA the 5′- and 3′-ends of each cDNA to the point in the coding sequence one codon beyond the fourth predicted transmembrane segment. PCR products of predicted sizes were obtained and gel purified. Heteromeric mixtures of PCR products, i.e., 5′-end of TASK-1 mixed with 3′-end of TASK-2 and vice versa, were made and amplified by PCR to produce a full-length clone by adding one primer designed against the 5′-end of the 5′ fragment and a comeback primer designed against the 3′-end of the other 3′ fragment. Successful PCR generated products of approximately 1500 base pairs; these products were subcloned into the pOX oocyte expression vector, and their chimeric compositions were confirmed by DNA sequencing across the fusion point. The chimeric cRNAs were also injected into *Xenopus* oocytes undergoing the same experimental protocols as TASK-1 and TASK-2 cRNA-injected oocytes. To show additional evidence of functional expression of these chimeric 2P K^+ channel subunits, the regulation of their activity by external pH was examined by superfusing oocytes injected with chimeric cRNAs with FR solution at different pH values.

Results

Agent-Specific and Dose-Dependent Local Anesthetic Inibition. Racemic bupivacaine and ropivacaine both reversibly inhibited TASK-2 currents in a concentration-dependent manner (Fig. 1, A and B). Concentration-inhibition experiments resulted in IC_{50} values of 26 (22–31) μM for bupivacaine and 95 (84–106) μM for ropivacaine. The Hill coefficients (n_H) were close to unity (0.8 and 1.0, respectively), thereby suggesting a single local anesthetic binding site in TASK-2. However, in contrast to the amide local anesthetics bupivacaine and ropivacaine, TASK-2 currents were much less sensitive to the lipid-soluble ester-linked local anesthetic tetracaine, with an IC_{50} of 1670 (763–3652) μM (Fig. 1C). TASK-2 currents were also quite insensitive to a 1 mM concentration of the ester-linked local anesthetic chloroprocaine (normalized response 0.86 ± 0.01, $n = 3$, Fig. 1D). A 1 mM concentration of lidocaine inhibited TASK-2 currents by 55 ± 4% ($n = 6$), whereas the same concentration of its quaternary positively charged analog QX314 had no effect ($n = 5$, Fig. 1D). The neutral local anesthetic benzocaine (1 mM) inhibited TASK-2 currents by only 16 ± 2% ($n = 6$, Fig. 1D). However, this result may somewhat underestimate the effect of benzocaine because ethanol 0.1% (vehicle control for benzocaine experiments) slightly potentiated TASK-2 currents (normalized response 1.18 ± 0.04, $n = 6$).

Stereoselective Local Anesthetic Inhibition. Figure 2A shows original recordings from a TASK-2 cRNA-injected oocyte obtained under control conditions and in the presence of 10 μM *S*-(−)-bupivacaine and 10 μM *R*-(+)-bupivacaine.

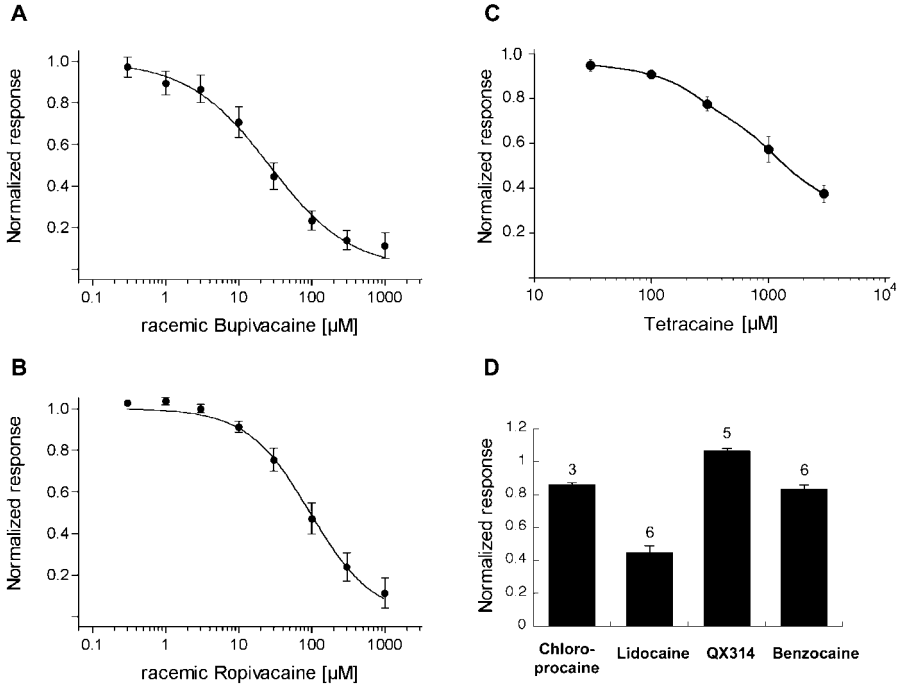

Fig. 1. Effects of different local anesthetics on TASK-2 currents. Concentration-response curves of TASK-2 currents for racemic bupivacaine (A) and racemic ropivacaine (B) are shown. Steady-state currents elicited by the depolarizing pulse of +40 mV have been normalized to control and fit to the Hill equation. IC_{50} values (95% confidence intervals) were for bupivacaine 26 (22–31) μM and for ropivacaine 95 (84–106) μM. The Hill coefficients (n_H) were 0.8 and 1.0, respectively. C, concentration-response curve of TASK-2 currents for the ester local anesthetic tetracaine is shown. Steady-state currents elicited by the depolarizing pulse of +40 mV have been normalized to control and fit to the Hill equation. The IC_{50} value (95% confidence interval) was 1670 (763–3652) μM and the Hill coefficient (n_H) was 1.0. Note that the *x*-axis in A, B, and C is represented as a log scale. D, normalized responses elicited by the depolarizing pulse of +40 mV of TASK-2 cRNA-injected oocytes to 1 mM chloroprocaine, 1 mM lidocaine, 1 mM QX314, and 1 mM benzocaine. Data are shown as mean ± S.E.M. Numbers above error bars refer to number of oocytes studied.

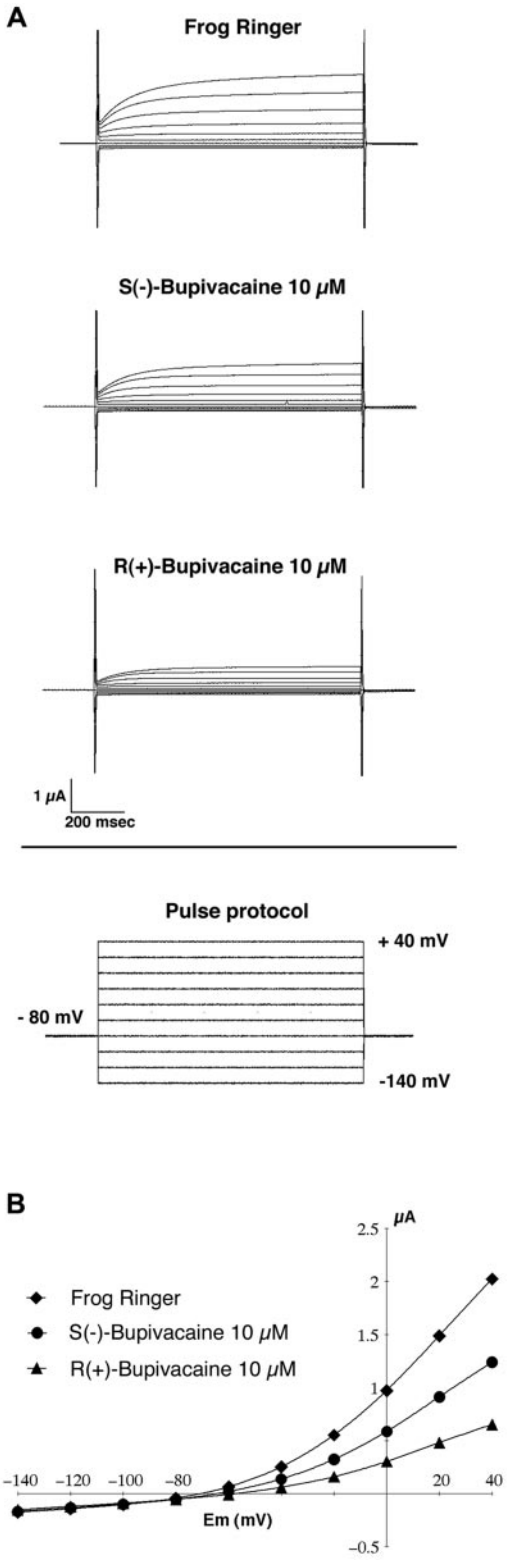

Fig. 2. Stereoselective effects of the enantiomers of bupivacaine on TASK-2 currents. A, representative raw current recordings from a TASK-2 cRNA-injected oocyte under control condition (frog Ringer's solution) and during application of 10 μM *S*-(−)-bupivacaine or 10 μM *R*-(+)-bupivacaine. Voltage pulses ranged from −140 mV to +40 mV in 20-mV increments from a holding potential of −80 mV. B, steady-state current-voltage curves of TASK-2 cRNA-injected oocytes in the presence or absence of 10 μM *R*-(+)-bupivacaine or 10 μM *S*-(−)-bupivacaine. The local anesthetic inhibition was not voltage-dependent as analyzed by the Woodhull model (see eq. 2, *Materials and Methods*).

At 10 μM, each enantiomer inhibited TASK-2 currents; *R*-(+)-bupivacaine was more potent than *S*-(−)-bupivacaine (normalized response 0.41 ± 0.02 measured at +40 mV, n = 9, versus 0.66 ± 0.04, n = 10, respectively; $p < 0.001$). The effects of both enantiomers were reversible upon superfusion of the oocytes with drug-free FR solution (data not shown). Figure 2B shows current-voltage relationships of TASK-2 cRNA-injected oocytes in control conditions and in the presence of 10 μM *S*-(−)-bupivacaine and 10 μM *R*-(+)-bupivacaine. Both enantiomers decreased the amplitude of the currents at membrane potentials positive to −40 mV. Although the inhibition of the currents was slightly more pronounced at more positive membrane potentials, fitting the Woodhull model to the data (see eq. 2, *Materials and Methods*) revealed a Woodhull coefficient δ that was not significantly different from zero (δ = 0.04). Concentration-response curves for both enantiomers revealed that *R*-(+)-bupivacaine is 2.5-fold more potent than *S*-(−)-bupivacaine [IC_{50} values with 95% confidence intervals were 17 (16–19) μM versus 43 (37–50) μM, respectively] (Fig. 3A). Similarly, *R*-(+)-ropivacaine was 2.8-fold more potent than *S*-(−)-ropivacaine [IC_{50} values 85 (76–95) μM versus 236 (211–263) μM, respectively] (Fig. 3B).

Activation Kinetics. Under control conditions, TASK-2 currents display a time-dependent activation (time constant τ = 147 ± 5 ms, measured at +40 mV, n = 5, and τ = 120 ± 9 ms, measured at −20 mV, n = 7) and are noninactivating over the entire pulse period (1 s), as previously described (Reyes et al., 1998; Gray et al., 2000). The time constant of the activation process was significantly lower at higher drug concentrations [τ = 96 ± 8 ms for 100 μM *S*-(−)-bupivacaine, n = 5, versus 134 ± 14 ms for 3 μM *S*-(−)-bupivacaine, n = 5, measured at +40 mV; $p < 0.05$]. However, the effect of bupivacaine on the activation time constant was not stereoselective [τ = 113 ± 6 ms for 10 μM *S*-(−)-bupivacaine, n = 4, versus 109 ± 6 ms for 10 μM *R*-(+)-bupivacaine, n = 4, measured at + 40 mV; $p > 0.05$].

Single-Channel Openings. Cell-attached patches from cells transfected with an expression plasmid coding for TASK-2 showed noninactivating baseline channels that conducted outward currents at depolarized potentials and inward currents at hyperpolarized potentials (Fig. 4A). This pattern of channel activity was not observed in sham transfected or untransfected cells. The application of racemic bupivacaine (100 μM) caused a rapid decrease in channel activity and open probability (P_o) that returned to the control state with washout (Fig. 4B). The average control P_o of TASK-2 currents before bupivacaine was 20.8 ± 1.6%, which decreased by 73% to 5.6 ± 2.2% in the presence of 100 μM racemic bupivacaine.

Membrane Depolarization. Oocytes that expressed TASK-2 had more negative resting membrane potentials than did water-injected control oocytes (for TASK-2, −76.5 ± 2.2 mV and for control, −49.0 ± 1 mV; $p < 0.001$). Bupivacaine caused an immediate and reversible depolarization of the membrane potential of oocytes expressing TASK-2 channels. Figure 5A shows tracings of membrane potentials before, during, and after treatment with 300 μM *R*-(+)-bupivacaine of TASK-2 cRNA-injected or water-injected oocytes. The bupivacaine-induced depolarization of TASK-2 cRNA-injected oocytes (15.8 ± 2.5 mV, n = 6) was significantly greater than the corresponding depolarization of water-injected control oocytes (0.1 ± 0.05 mV, n = 4; $p < 0.001$) (Fig.

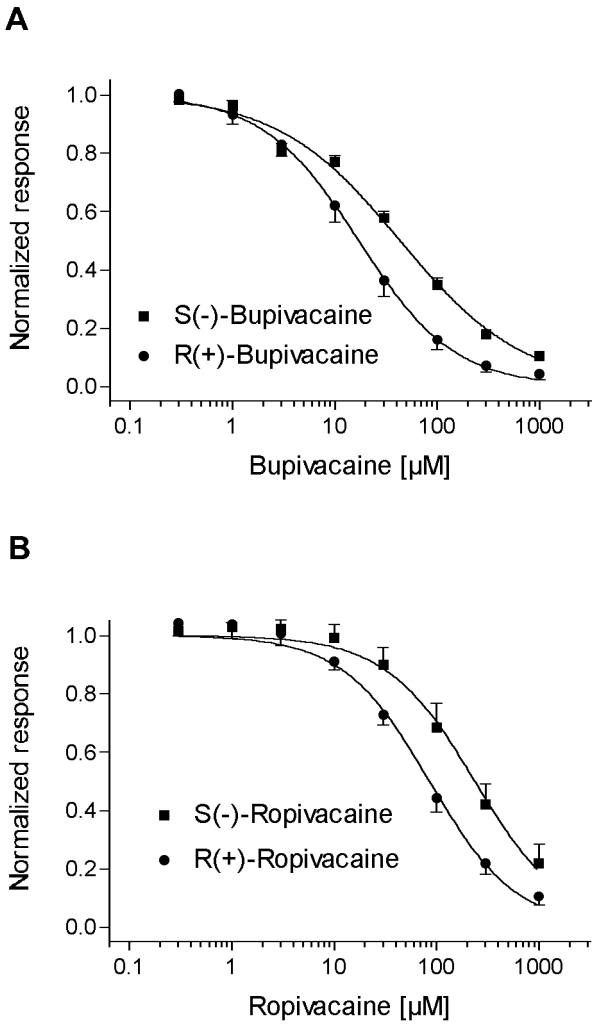

Fig. 3. A, concentration-response curves of TASK-2 currents for *R*-(+)-bupivacaine (filled circles) and *S*-(−)-bupivacaine (filled squares) are shown. IC_{50} values (95% confidence intervals) were for *R*-(+)-bupivacaine 17 (16–19) μM and for *S*-(−)-bupivacaine 43 (37–50) μM. The Hill coefficients (n_H) were 0.9 and 0.7, respectively. B, concentration-response curves of TASK-2 currents for *R*-(+)-ropivacaine (filled circles) and *S*-(−)-ropivacaine (filled squares) are shown. IC_{50} values (95% confidence intervals) were for *R*-(+)-ropivacaine 85 (76–95) μM and for *S*-(−)-ropivacaine 236 (211–263) μM. The Hill coefficients (n_H) were 1.0 and 1.1, respectively. Steady-state currents elicited by the depolarizing pulse of +40 mV have been normalized to control and fit to the Hill equation. Note that the *x*-axis in A and B is represented as a log scale.

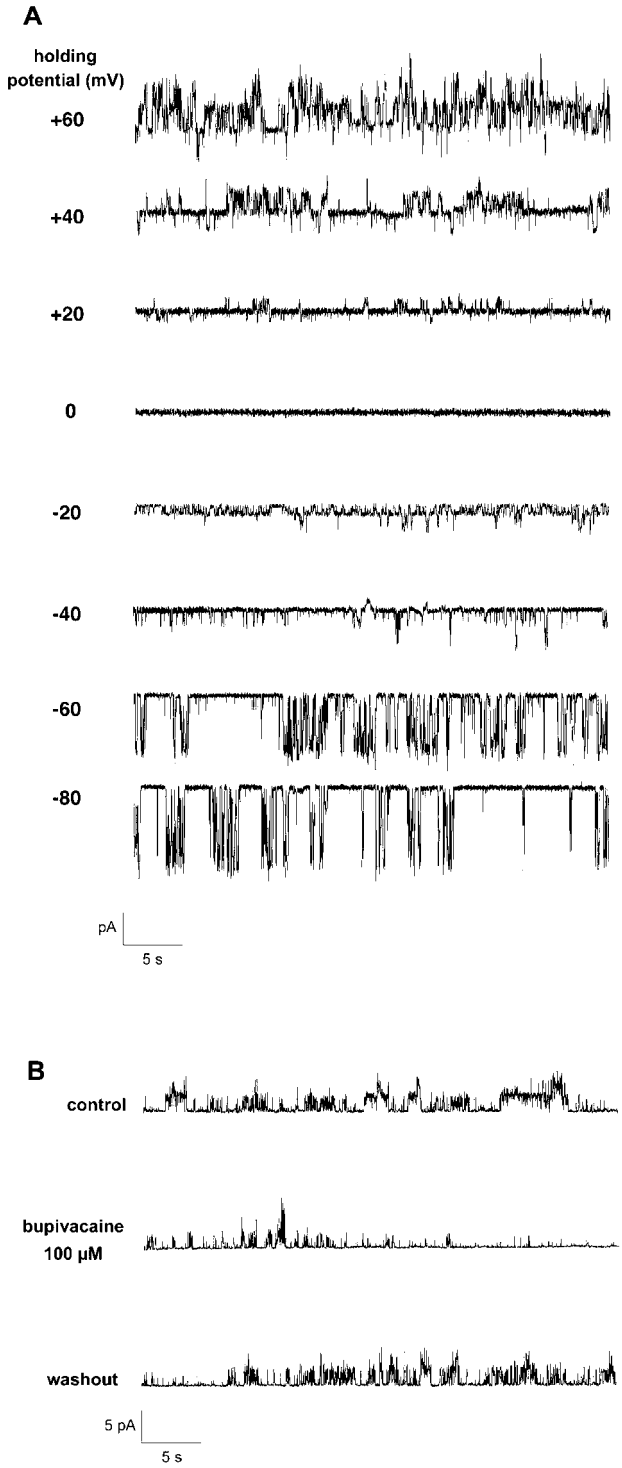

Fig. 4. Patch-clamp recordings of TASK-2 currents expressed in HEK 293 cells. A, unitary TASK-2 currents from on-cell patches at several holding potentials. The recording pipette was filled with 150 mM potassium-aspartate, and the currents were filtered at 2 kHz. B, shown are single-channel recordings of TASK-2 in control condition, in response to exposure to 100 μM racemic bupivacaine, decreasing channel open probability by 73%, from 20.8 ± 1.6% to 5.6 ± 2.2%, and following washout (holding potential +40 mV).

5B). The small depolarizations by 300 μM bupivacaine observed in water-injected oocytes may be explained by inhibition of endogenous background K^+ channels.

Chimeric TASK-1/TASK-2 Channels. Oocytes injected with the chimeric cRNAs of TASK-1/TASK-2 (chimera1) and TASK-2/TASK-1 (chimera2) subunits (Fig. 6A) displayed typical noninactivating outward currents at depolarized potentials as previously described for wild-type TASK-1 (Duprat et al., 1997; Leonoudakis et al., 1998) and TASK-2 (Reyes et al., 1998; Gray et al., 2000) that were not present in control oocytes. Both chimeric subunits remained as sensitive to changes in external pH as wild-type TASK-1 (pH_m 7.3) and TASK-2 (pH_m 7.8) (Duprat et al., 1997; Reyes et al., 1998), showing potentiation of currents at extracellular pH >7.6 and significant inhibition at extracellular pH <7.0 (Fig. 6B). Like their wild-type parents, both chimeric subunits were inhibited by bupivacaine in the low micromolar range. However, the C-terminal tail of TASK-2 appeared to confer greater bupivacaine sensitivity when present in a subunit. The IC_{50} of bupivacaine for TASK-1 was reduced approxi-

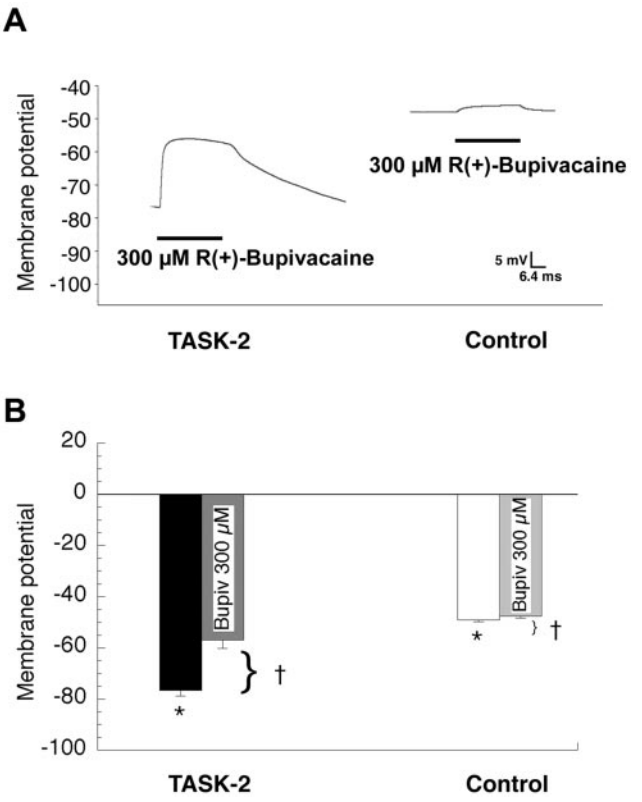

Fig. 5. Depolarization of TASK-2 cRNA-injected or water-injected control oocytes during exposure to bupivacaine. A, representative tracings of the resting membrane potentials before, during, and after treatment with 300 μM *R*-(+)-bupivacaine. Bupivacaine was applied for 30 s (horizontal bars). B, depolarization, in millivolts, of both TASK-2 cRNA-injected (n = 6) and water-injected control oocytes (n = 4). Data are expressed as mean ± S.E.M. ⋆, $p < 0.001$, difference of the resting membrane potential between TASK-2 cRNA-injected and water-injected control oocytes. †, $p < 0.001$, difference of the bupivacaine-induced depolarization between TASK-2 cRNA-injected and control oocytes.

mately by half with the introduction of the TASK-2 tail [chimera1, bupivacaine IC_{50} = 33 μM compared with TASK-1, 68 μM (Leonoudakis et al., 1998)]. Correspondingly, replacing the C-terminal tail of TASK-2 with a TASK-1 tail (chimera2) increased the IC_{50} approximately 3-fold [chimera2, bupivacaine IC_{50} = 86 μM compared with TASK-2, 26 μM; Fig. 6C)].

Interestingly, chimera2 currents displayed a change in activation kinetics compared with its wild-type parent TASK-2 (Fig. 6D). As described previously, TASK-2 currents activate slowly following a voltage jump (Reyes et al., 1998; Gray et al., 2000), whereas TASK-1 currents are almost fully activated instantaneously (Duprat et al., 1997; Leonoudakis et al., 1998). This difference can be described as the fractional instantaneous current present shortly (150 ms) after the voltage jump. In the present studies, TASK-1 and chimera1 displayed nearly full fractional instantaneous currents [TASK-1 94.4 ± 0.4% (n = 10); chimera1 94.1 ± 0.5% (n = 10)] and TASK-2 displayed its typical delayed activation [44.0 ± 0.8% (n = 10)]. Chimera2, in which the native TASK-2 C-terminal tail has been replaced by the tail of TASK-1, showed an intermediate pattern of activation [fractional instantaneous current 66.9 ± 0.6% (n = 10)] that was significantly different from that of either TASK-1 or TASK-2 ($p < 0.001$).

Discussion

Local anesthetics inhibit voltage-gated K^+ channels (González et al., 2001b), G protein-coupled inward rectifying K^+ channels (Zhou et al., 2001), and the 2P K^+ channels TASK-1, TASK-3, and TREK-1 (Kindler et al., 1999; Kim et al., 2000). The present study reports potent, agent-selective local anesthetic inhibition of the 2P K^+ channel TASK-2 with both whole-cell and single-channel recording techniques. Although TASK-2 shares only 27% and 26% amino acid sequence identity with TASK-1 and TASK-3, it belongs to the subfamily of acid-sensitive 2P K^+ channels; however, its sensitivity for extracellular pH is less steep than that for TASK-1 or TASK-3. With the IC_{50} values for bupivacaine and ropivacaine in the low micromolar range, TASK-2 is the most sensitive 2P K^+ channel to local anesthetics. The IC_{50} for TASK-2 bupivacaine inhibition is in the range of the high-affinity binding of the drug to the inactivated state of the cardiac Na^+ channel (~1 μM) (Clarkson and Hondeghem, 1985). We observed a distinct local anesthetic agent specificity for TASK-2 inhibition. The ester-linked local anesthetic tetracaine, which is also highly lipid-soluble, was a much weaker inhibitor of TASK-2 currents (IC_{50} >1 mM) than the amide local anesthetics bupivacaine and ropivacaine. Chloroprocaine, another ester-linked local anesthetic, had almost no effect on TASK-2 currents. Although hydrophobic sites are important determinants of local anesthetic inhibition, the observed resistance of TASK-2 to ester-linked local anesthetics implies that structural elements contribute to the potency of inhibition. This agent-specific inhibition for TASK-2 is very similar to that previously described for the physiological flicker channel in frog myelinated axons (Bräu et al., 1995). TASK-2 shares many electrophysiological and pharmacological properties with this physiological background K^+ channel, with the significant exception that the IC_{50} of *R*-(+)-bupivacaine for TASK-2 (17 μM) is approximately 100 times higher than that reported for the flicker channel (0.15 μM) (Nau et al., 1999a).

Whereas TASK-1 lacks a stereoselective effect of local anesthetics (Kindler et al., 1999), TASK-2 showed a stereoselective ratio (*R*/*S*) for bupivacaine and ropivacaine of ~3. Optically pure enantiomers of local anesthetics have now been introduced into clinical practice as less toxic alternatives to racemic mixtures (Huang et al., 1998). The magnitude of stereoselectivity of TASK-2 inhibition by bupivacaine and ropivacaine is comparable both to the reported selectivity of inhibition of the inactivated states of voltage-gated Na^+ channels (Valenzuela et al., 1995b) and to the higher systemic toxicity for *R*-(+)-bupivacaine in animal studies (Aberg, 1972). This stereoselective local anesthetic inhibition makes TASK-2 a potential molecular target in vivo for both the action and side effects of local anesthetics. The observed *R*/*S* ratio for TASK-2 also is similar to the recently reported stereoselective effect of the new local anesthetic IQB-9302 on the human cardiac K^+ channel hKv1.5 (*R*/*S* ratio ~3.2) (González et al., 2001a). Higher stereoselectivity has only been reported for bupivacaine inhibition of hKv1.5 (*R*/*S* ratio ~7) (Valenzuela et al., 1995a) and the flicker channel (*R*/*S* ratio ~73) (Nau et al., 1999a). Residues within the sixth transmembrane domain appear critical for stereoselective inhibition of both hKv1.5 (Franqueza et al., 1997) and Na^+ channels (Nau et al., 1999b). However, major structural dif-

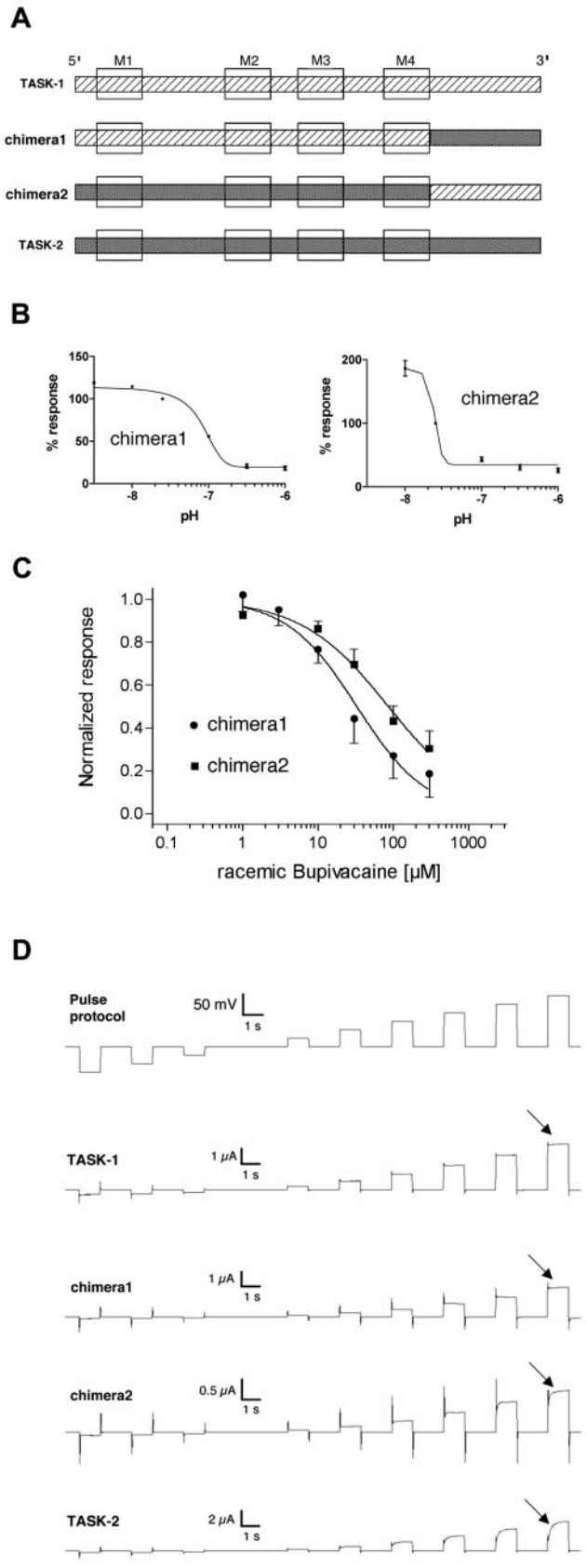

Fig. 6. A, chimeric TASK-1/TASK-2 (chimera1) and TASK-2/TASK-1 (chimera2) 2P K^+ channel subunits were produced by nested, sequential PCR to exchange the C-terminal intracellular domains of TASK-1 with TASK-2. Relative contributions from each of the parent wild-type channel subunits are shown. M1 to M4 indicate transmembrane domains. B, effect of extracellular pH on currents from oocytes expressing chimera1 or chimera2 subunits. Steady-state currents elicited by the depolarizing pulse of +40 mV have been normalized to control and fit to the Hill equation. C, effects of racemic bupivacaine on chimeric TASK-1/TASK-2 (chimera1, filled circles) and TASK-2/TASK-1 (chimera2, filled squares) 2P K^+ channel subunits. Concentration-response curves for bupivacaine are shown. The IC_{50} (95% confidence interval) of bupivacaine for chimera1 was 33 (26–41) μM and for chimera2 it was 86 (69–107) μM. Steady-state currents elicited by the depolarizing pulse of +40 mV have been normalized to control and fit to the Hill equation. Note that the *x*-axis in B and C is represented as a log scale. D, representative raw current recordings showing activation kinetics of TASK-1, TASK-2, chimera1, and chimera2 currents (voltage pulses ranged from −140 mV to +40 mV in 20-mV increments from a holding potential of −80 mV). TASK-1 and chimera1 display nearly complete instantaneous activation, whereas TASK-2 shows time-dependent activation (arrows). Chimera2 shows an activation profile intermediate to TASK-1 and TASK-2.

ferences exist between background 2P K^+ channels and voltage-gated K^+ and Na^+ channels, preventing identification of homologous sites in TASK-2. Analysis of single-channel recordings of TASK-2 expressed in HEK 293 cells showed that racemic bupivacaine decreased open probability, whereas single-channel current amplitudes and number of channels in the patch remained unchanged.

Local anesthetics depolarize cells expressing TASK-2 channels (Fig. 5); this effect could play a role in local anesthetic mechanisms. Since local anesthetics preferentially bind to the inactivated states of Na^+ channels that predominate at depolarized membrane potentials (Hille et al., 1975), inhibition of background K^+ channels could increase the binding of local anesthetics to Na^+ channels and enhance action potential blockade by causing partial depolarization and, therefore, promoting Na^+ channel inactivation. Previous experimental evidence supports this hypothesis; myelinated nerves exhibiting physiological background K^+ channel activity do depolarize in response to local anesthetics (Bräu et al., 1995), and background K^+ channels have been shown to control the resting membrane potential of several neuronal cells (Jones, 1989). In addition, inhibition of background K^+ channels may contribute to cardiotoxic and excitotoxic side effects of local anesthetics, which cannot be entirely explained by inhibition of Na^+ channels alone. Inhibition of K^+ channels increases membrane excitability, which could contribute to local anesthetic-induced arrhythmias and convulsions (Zhou et al., 2001). This potential mechanism is supported by the finding that K^+ channel openers reverse bupivacaine cardiotoxicity (de La Coussaye et al., 1993). Local anesthetic inhibition of the acid-sensitive 2P K^+ channels TASK-1 and TASK-2, both expressed in heart and CNS, occurs in the range of arterial plasma levels that are associated with local anesthetic toxicity (Kindler et al., 1999).

Many modulatory effects described for 2P K^+ channels occur via the C-terminal domain of the respective channel; for example, activation of TASK-1 by volatile anesthetics (Talley and Bayliss, 2002), sensitivity to arachidonic acid of TREK-2 (Kim et al., 2001), and inhibition of TASK-1 by the transmitter thyrotropin-releasing hormone (Talley and Bayliss, 2002) are dependent on an intact C-terminal tail. Our previous attempts to produce C-terminal truncation mutants of TASK-2 at amino acid positions 252 and 278 failed to produce functional ion channel activity (Gray et al., 2000). Therefore, in the present study we constructed chimeric TASK-1/TASK-2 and TASK-2/TASK-1 2P K^+ channel subunits by switching the C-terminal domains to the other 2P

K^+ channel. The finding that the sensitivity to bupivacaine of each chimera was influenced by the presence of the predicted intracellular C-terminal domain of TASK-2 implies that it plays a role in local anesthetic modulation. Furthermore, the permanently charged lidocaine derivative QX314 had no effect on TASK-2 currents, implying an intracellular or membrane site of action. Given that the neutral local anesthetic benzocaine was also a poor inhibitor of TASK-2, we suggest that both the ionized and un-ionized forms of local anesthetics participate in TASK-2 inhibition, the uncharged species to achieve cellular penetration and the charged form to act at an intracellular or membrane site.

The activation patterns shown by the chimeric TASK channels suggest that the C-terminal tail of TASK-2 also may contribute to the delayed activation, but is not sufficient by itself. Replacing the TASK-2 C-terminal with the TASK-1 C-terminal (chimera2) significantly reduced delayed activation (fractional instantaneous current 67% for chimera2 versus 44% for TASK-2), whereas replacing the TASK-1 C-terminal with the TASK-2 C-terminal (chimera1) had no effect on activation (fractional instantaneous current 94% for chimera1 versus 94% for TASK-1) (Fig. 6D). Mutational experiments of the yeast 2P K^+ channel TOK1 identified regions at the cytoplasmic ends of the transmembrane segments following either of the duplicated pore loops to be important for gating of TOK1 (Loukin et al., 1997). However, poor overall homology between TASK-2 and TOK1 (only 12% amino acid identity) and the presence of eight transmembrane segments in TOK1 compared with only four in TASK-2 make accurate alignments of the protein sequences of TASK-2 and TOK1 impossible.

In summary, we report potent, agent-specific, and stereoselective local anesthetic inhibition of the human 2P K^+ channel TASK-2. Whether TASK-2 represents the mammalian homolog of the amphibian background K^+ channel termed flicker channel will need further studies including expression experiments in peripheral nerves. The differences of the potency of the bupivacaine enantiomers and the *R*/*S* ratio between TASK-2 and the flicker channel could reflect species-specific variation of closely related ion channels. However, the discrepancy between these results may also be explained by differences in expression systems, such as different post-translational modifications or accessory subunits.

Acknowledgments

We thank Elizabeth Sampson and Frank Shen for expert technical assistance and Joan Etlinger for editorial advice. We also thank Dr. Dag Selander, AstraZeneca, Sweden, for kindly providing us with the enantiomers of bupivacaine and ropivacaine.

References

Aberg G (1972) Toxicological and local anaesthetic effects of optically active isomers of two local anaesthetic compounds. *Acta Pharmacol Toxicol* **31:**273–286.

Aimond F, Rauzier JM, Bony C, and Vassort G (2000) Simultaneous activation of p38 MAPK and p42/44 MAPK by ATP stimulates the K^+ current ITREK in cardiomyocytes. *J Biol Chem* **275:**39110–39116.

Barbuti A, Ishii S, Shimizu T, Robinson RB, and Feinmark SJ (2002) Block of the background K(+) channel TASK-1 contributes to arrhythmogenic effects of platelet-activating factor. *Am J Physiol* **282:**H2024–H2030.

Bräu ME, Nau C, Hempelmann G, and Vogel W (1995) Local anesthetics potently block a potential insensitive potassium channel in myelinated nerve. *J Gen Physiol* **105:**485–505.

Bräu ME, Vogel W, and Hempelmann G (1998) Fundamental properties of local anesthetics: half-maximal blocking concentrations for tonic block of Na+ and K+ channels in peripheral nerve. *Anesth Analg* **87:**885–889.

Bushell T, Clarke C, Mathie A, and Robertson B (2002) Pharmacological characterization of a non-inactivating outward current observed in mouse cerebellar Purkinje neurones. *Br J Pharmacol* **135:**705–712.

Butterworth JF and Strichartz GR (1990) Molecular mechanisms of local anesthesia: a review. *Anesthesiology* **72:**711–734.

Clarkson CW and Hondeghem LM (1985) Mechanism for bupivacaine depression of cardiac conduction: fast block of sodium channels during the action potential with slow recovery from block during diastole. *Anesthesiology* **62:**396–405.

de La Coussaye JE, Eledjam JJ, Peray P, Bruelle P, Lefrant JY, Bassoul B, Desch G, Gagnol JP, and Sassine A (1993) Lemakalim, a potassium channel agonist, reverses electrophysiological impairments induced by a large dose of bupivacaine in anaesthetized dogs. *Br J Anaesth* **71:**534–539.

Drachman D and Strichartz G (1991) Potassium channel blockers potentiate impulse inhibition by local anesthetics. *Anesthesiology* **75:**1051–1061.

Duprat F, Lesage F, Fink M, Reyes R, Heurteaux C, and Lazdunski M (1997) TASK, a human background K+ channel to sense external pH variations near physiological pH. *EMBO (Eur Mol Biol Organ) J* **16:**5464–5471.

Eglen RM, Hunter JC, and Dray A (1999) Ions in the fire: recent ion-channel research and approaches to pain therapy. *Trends Pharmacol Sci* **20:**337–342.

Franqueza L, Longobardo M, Vicente J, Delpón E, Tamkun MM, Tamargo J, Snyders DJ, and Valenzuela C (1997) Molecular determinants of stereoselective bupivacaine block of hKv1.5 channels. *Circ Res* **81:**1053–1064.

Gabriel A, Abdallah M, Yost CS, Winegar BD, and Kindler CH (2002) Localization of the tandem pore domain K+ channel KCNK5 (TASK-2) in the rat central nervous system. *Mol Brain Res* **98:**153–163.

Goldstein SA, Bockenhauer D, O'Kelly I, and Zilberberg N (2001) Potassium leak channels and the KCNK family of two-P-domain subunits. *Nat Rev Neurosci* **2:**175–184.

González T, Longobardo M, Caballero R, Delpón E, Sinisterra JV, Tamargo J, and Valenzuela C (2001a) Stereoselective effects of the enantiomers of a new local anaesthetic, IQB-9302, on a human cardiac potassium channel (Kv1.5). *Br J Pharmacol* **132:**385–392.

González T, Longobardo M, Caballero R, Delpón E, Tamargo J, and Valenzuela C (2001b) Effects of bupivacaine and a novel local anesthetic, IQB-9302, on human cardiac K+ channels. *J Pharmacol Exp Ther* **296:**573–583.

Gray AT, Zhao BB, Kindler CH, Winegar BD, Mazurek MJ, Xu J, Chavez RA, Forsayeth JR, and Yost CS (2000) Volatile anesthetics activate the human tandem pore domain baseline K+ channel KCNK5. *Anesthesiology* **92:**1722–1730.

Hille B, Courtney K, and Dum R (1975) Rate and site of local anesthetics in myelinated nerve fibers, in *Progress in Anesthesiology. Molecular Mechanisms of Anesthesia* (Fink BR ed) pp 13–20, Raven Press Publishers, New York.

Huang YF, Pryor ME, Mather LE, and Veering BT (1998) Cardiovascular and central nervous system effects of intravenous levobupivacaine and bupivacaine in sheep. *Anesth Analg* **86:**797–804.

Jones SW (1989) On the resting potential of isolated frog sympathetic neurons. *Neuron* **3:**153–161.

Kim Y, Bang H, Gnatenco C, and Kim D (2001) Synergistic interaction and the role of C-terminus in the activation of TRAAK K+ channels by pressure, free fatty acids and alkali. *Pfluegers Arch Eur J Physiol* **442:**64–72.

Kim Y, Bang H, and Kim D (2000) TASK-3, a new member of the tandem pore K+ channel family. *J Biol Chem* **275:**9340–9347.

Kindler CH, Yost CS, and Gray AT (1999) Local anesthetic inhibition of baseline potassium channels with two pore domains in tandem. *Anesthesiology* **90:**1092–1102.

Komai H and McDowell TS (2001) Local anesthetic inhibition of voltage-activated potassium currents in rat dorsal root ganglion neurons. *Anesthesiology* **94:**1089–1095.

Kotelko DM, Shnider SM, Dailey PA, Brizgys RV, Levinson G, Shapiro WA, Koike M, and Rosen MA (1984) Bupivacaine-induced cardiac arrhythmias in sheep. *Anesthesiology* **60:**10–18.

Leonoudakis D, Gray AT, Winegar BD, Kindler CH, Harada M, Taylor DM, Chavez RA, Forsayeth JR, and Yost CS (1998) An open rectifier potassium channel with two pore domains in tandem cloned from rat cerebellum. *J Neurosci* **18:**868–877.

Loukin SH, Vaillant B, Zhou X-L, Spalding EP, Kung C, and Saimi Y (1997) Random mutagenesis reveals a region important for gating of the yeast K+ channel Ykc1. *EMBO (Eur Mol Biol Organ) J* **16:**4817–4825.

Millar JA, Barratt L, Southan AP, Page KM, Fyffe RE, Robertson B, and Mathie A (2000) A functional role for the two-pore domain potassium channel TASK-1 in cerebellar granule neurons. *Proc Natl Acad Sci USA* **97:**3614–3618.

Nau C, Vogel W, Hempelmann G, and Bräu ME (1999a) Stereoselectivity of bupivacaine in local anesthetic-sensitive ion channels of peripheral nerve. *Anesthesiology* **91:**786–795.

Nau C, Wang SY, Strichartz GR, and Wang GK (1999b) Point mutations at N434 in D1–S6 of mu1 Na(+) channels modulate binding affinity and stereoselectivity of local anesthetic enantiomers. *Mol Pharmacol* **56:**404–413.

Olschewski A, Hempelmann G, Vogel W, and Safronov BV (1998) Blockade of Na+ and K+ currents by local anesthetics in the dorsal horn neurons of the spinal cord. *Anesthesiology* **88:**172–179.

Ragsdale DS, McPhee JC, Scheuer T, and Catterall WA (1994) Molecular determinants of state-dependent block of Na+ channels by local anesthetics. *Science (Wash DC)* **265:**1724–1728.

Reyes R, Duprat F, Lesage F, Fink M, Salinas M, Farman N, and Lazdunski M (1998) Cloning and expression of a novel pH-sensitive two pore domain K+ channel from human kidney. *J Biol Chem* **273:**30863–30869.

Talley EM and Bayliss DA (2002) Modulation of TASK-1 (Kcnk3) and TASK-3 (Kcnk9) potassium channels. Volatile anesthetics and neurotransmitters share a molecular site of action. *J Biol Chem* **277:**17733–17742.

Talley EM, Solorzano G, Lei Q, Kim D, and Bayliss DA (2001) Cns distribution of members of the two-pore-domain (KCNK) potassium channel family. *J Neurosci* **21:**7491–7505.

Terrenoire C, Lauritzen I, Lesage F, Romey G, and Lazdunski M (2001) A TREK-1-

like potassium channel in atrial cells inhibited by beta-adrenergic stimulation and activated by volatile anesthetics. *Circ Res* **89:**336–342.
Valenzuela C, Delpón E, Tamkun MM, Tamargo J, and Snyders DJ (1995a) Stereoselective block of a human cardiac potassium channel (Kv1.5) by bupivacaine enantiomers. *Biophys J* **69:**418–427.
Valenzuela C, Snyders DJ, Bennett PB, Tamargo J, and Hondeghem LM (1995b) Stereoselective block of cardiac sodium channels by bupivacaine in guinea pig ventricular myocytes. *Circulation* **92:**3014–3024.
Zhou W, Arrabit C, Choe S, and Slesinger PA (2001) Mechanism underlying bupivacaine inhibition of G protein-gated inwardly rectifying K+ channels. *Proc Natl Acad Sci USA* **98:**6482–6487.

Address correspondence to: Dr. Christoph H. Kindler, Attending Physician, Department of Anesthesia, University Clinics, Kantonsspital, CH-4031 Basel, Switzerland. E-mail: ckindler@uhbs.ch